JOC The Journal of Organic Chemistry

Article

pubs.acs.org/joc

Synthesis, Basicity, Structural Characterization, and Biochemical Properties of Two [(3-Hydroxy-4-pyron-2-yl)methyl]amine Derivatives Showing Antineoplastic Features.

Stefano Amatori,[†] Gianluca Ambrosi,[‡] Mirco Fanelli,*[,†] Mauro Formica,[‡] Vieri Fusi,[‡,*] Luca Giorgi,[‡] Eleonora Macedi,[§] Mauro Micheloni,[‡] Paola Paoli,*[,§] Roberto Pontellini,[‡] and Patrizia Rossi[§]

[†]Molecular Pathology and Oncology Laboratory "PaoLa", Department of Biomolecular Sciences, University of Urbino, via Arco d'Augusto 2, I-61032 Fano (PU), Italy

[‡]Department of Basic Sciences and Fundamentals, University of Urbino, P.za Rinascimento 6, I-61029 Urbino, Italy

[§]Department of Energy Engineering "Sergio Stecco", University of Florence, Via S. Marta 3, I-50139 Florence, Italy

Supporting Information

ABSTRACT: The *N*,*N*′-bis[(3-hydroxy-4-pyron-2-yl)methyl]-*N*,*N*′-dimethylethylendiamine (malten) and 4,10-bis[(3-hydroxy-4-pyron-2-yl)methyl]-1,7-dimethyl-1,4,7,10-tetraazacyclododecane (maltonis) were synthesized and characterized. The acid−base behavior, structural characterizations, and biochemical studies in aqueous solution were reported. Each compound contains two 3-hydroxy-2-methyl-4-pyrone units (maltol) symmetrically spaced by a polyamine fragment, the 1,4-dimethylethylendiamine (malten), or the 1,7-dimethyl-1,4,7,10-tetraazacyclododecane (maltonis). They are present at physiological pH 7.4 in the form of differently charged species: neutral but in a zwitterion form for malten and monopositive with an internal separation of charges for maltonis. Malten and maltonis are both able to alter the chromatin structure inducing the covalent binding of genomic DNA with proteins, a feature consistent with the known antiproliferative activity exerted by this class of molecules. Solid-state results and MD simulations in water show that malten, because of its molecular topology, should be more prone than maltonis to act as a donor of H-bonds in intermolecular contacts, thus it should give a better noncovalent approach with the negatively charged DNA. Crystal structures of $[H_2malten]^{2+}$ and $[H_2maltonis]^{2+}$ cations were also reported.

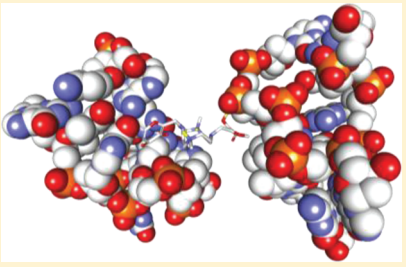

INTRODUCTION

New molecules for potential pharmacological uses are continuously synthesized, developed, and tested. Antineoplastic agents are one of the main targets because, although great progress has been made in the treatment of neoplastic diseases, the survival of patients affected by tumor remains in many cases very limited.[1] In these cases, the main problems are related to the lack of specific therapies as well as to the resistance to currently used chemotherapeutic drugs, which are furthermore cytotoxic, thus causing severe side effects. In this light, there is an urgent necessity to identify and synthesize new molecules showing both a higher effective and/or selective antitumor activity and increased human body tolerability.

Recently, we developed a new class of molecules based on the 3-hydroxy-2-methyl-4-pyrone unit (maltol, Chart 1), which exhibited antineoplastic activity in vitro.[2,3]

Maltol is a natural compound used in food, beverage, tobacco, brewing, and cosmetics for its flavor and antioxidant properties.[4] It exhibits interesting antineoplastic activities attributed to the formation of reactive oxygen species (ROS)[5] as well as coordination properties toward metal ions; for this reason, ligands containing maltol have been developed and exploited as new potential metal-based antitumor drugs.[6a−d] In addition, oxovanadium(IV) complexes of ligands based on maltol were developed by Orvig and co-workers as insulin-enhancing agents.[6e,f]

Linear and macrocyclic polyamines, generally with symmetrical topology, are also known antitumor agents.[7] With a goal to produce new anticancer agents, we developed a new class of maltol-derived molecules coupling maltol and polyamine symmetrically.[2] The newly designed compounds show two [(3-hydroxy-4-pyron-2-yl)methyl]amine units separated by different aliphatic spacers with or without a cyclic skeleton. The *N*,*N*′-bis((3-hydroxy-4-pyron-2-yl)methyl)-*N*,*N*′-dimethylethylendiamine (malten, Chart 1), showed antiproliferative activity in eight tumor cell lines. Malten exposure led to a dose-dependent reduction in cell survival in all of the neoplastic models studied, associated with the activation of programmed cell death (apoptosis) and cell cycle arrest. In accordance with biological studies, it was demonstrated that malten exposure modulates the expression of genes having key roles in cell cycle progression and apoptosis. Complex DNA structural modifications are induced by malten treatments, suggesting that a DNA intermolecular cross-linking activity could be part of the mechanism of action of the compound.[3] Interestingly, the key

Received: November 9, 2011
Published: February 1, 2012

dx.doi.org/10.1021/jo202270j | J. Org. Chem. 2012, 77, 2207−2218

Chart 1. Compounds Maltol, Malten, and Maltonis with Atom Labeling Used in NMR Assignments

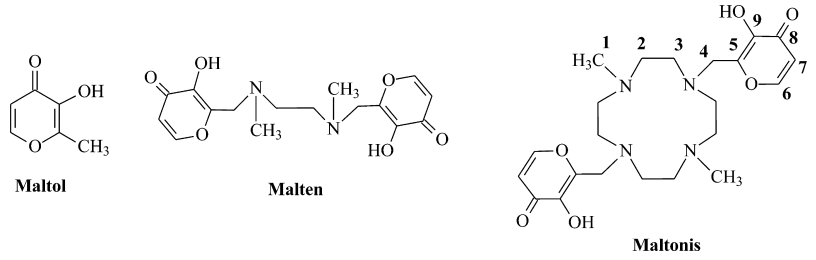

Scheme 1. Synthetic Pathway

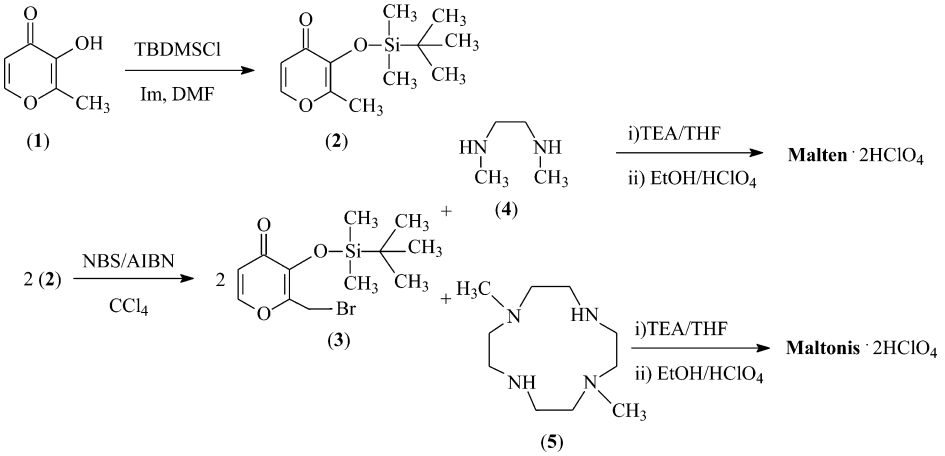

of the activity, compared to the previous maltol derivatives reported, seems to consist in the simultaneous presence of the two amino-spaced maltols.

It must be considered that these molecules show acid−base properties and can be present in solution in neutral form but also as anionic and cationic species, depending on the pH value. This aspect is of fundamental importance to better define the biologically active species.

For this reason, in addition to the detailed synthesis and chemical characterization of two molecules belonging to this class, *N*,*N*′-bis((3-hydroxy-4-pyron-2-yl)methyl)-*N*,*N*′-dimethylethylendiamine (malten) and 4,10-bis[(3-hydroxy-4-pyron-2-yl)methyl]-1,7-dimethyl-1,4,7,10-tetraazacyclododecane (maltonis, Chart 1), an exhaustive study concerning the acid−base properties, the structural conformation and proton distribution of these compounds is also reported. The crystal structures of the diprotonated species of malten and maltonis (**6** = $[H_2malten](ClO_4)_2{\cdot}2(H_2O)$, **7** = $[H_2maltonis](ClO_4)_2$) are reported as well as the results of theoretical studies directed to better understand the conformational space accessible to the two molecules and to study possible interaction paths between malten and maltonis and DNA. Finally, additional biological studies were carried out in tumor cellular models in order to further clarify the molecular mechanism through which both malten and maltonis exert their biological effect.

RESULTS AND DISCUSSION

Synthesis. *N*,*N*′-Bis[(3-hydroxy-4-pyron-2-yl)methyl]-*N*,*N*′-dimethylethylendiamine (malten) and 4,10-bis[(3-hydroxy-4-pyron-2-yl)methyl]-1,7-dimethyl-1,4,7,10-tetraazacyclododecane (maltonis) were synthesized following the procedure reported in Scheme 1. Reagent **3** was obtained from the commercial compound 2-methyl-3-hydroxy-4-pyrone (**1**, maltol) by methods reported in literature.[8] *N*,*N*′-Dimethylethylendiamine (**4**) is a commercial compound and was used without further purification, while polyamine 1,7-dimethyl-1,4,7,10-tetraazacyclododecane (**5**) was synthesized by following standard procedures reported in the literature.[9] The synthetic procedure includes the coupling of the maltol (**1**), appropriately protected (**2**), and activated (**3**) with the secondary amine present in reagent **4** or **5**. Reagent **3** was not isolated and was used freshly prepared without purification; 2 equiv of **3** was added compared with the polyamines **4** and **5**, each of them providing two secondary amine groups. The obtained crude products were treated with 10% perchloric acid ethanol solution to obtain the desired compounds malten and maltonis as hydroperchlorate salts in good yields. The acid treatment simultaneously allows the deprotection of the hydroxyl function and the cleansing of compounds, thus avoiding tedious and expensive chromatographic purifications. The two final products can be further purified by easy recrystallization using sodium perchlorate saturated water solution as nontoxic medium.

Basicity. Table 1 summarizes the basicity constants of malten and maltonis potentiometrically determined in 0.15 mol dm^{-3} NMe_4Cl aqueous solution at 298.1 K. Both neutral compounds L behave as diprotic acids, while neutral malten behaves as a diprotic and maltonis as a triprotic base under the experimental conditions used. In fact, as shown in Table 1, they can be present in solution as anionic species $H_{-2}L^{2-}$, indicating the removal of the acidic hydrogen atom of each maltol moiety while they can add up to two or three protons achieving H_2L^{2+} or H_3L^{3+}species for malten and maltonis, respectively.

By analyzing the protonation constants starting from the anionic $H_{-2}L^{2-}$ species, it was found that maltonis behaves as a stronger base than malten in each protonation step; this can be

dx.doi.org/10.1021/jo202270j | J. Org. Chem. 2012, 77, 2207−2218

Table 1. Protonation Constants (log K) of Malten and Maltonis Determined by Potentiometric Measurements in 0.15 mol dm^{-3} NMe_4Cl Aqueous Solution at 298.1 K

	log K	
reaction	L = malten	L = maltonis
$H_{-2}L^{2-} + H^+ = H_{-1}L^-$	9.03(1)[a]	11.08(1)
$H_{-1}L^- + H^+ = L$	7.86(1)	9.30(1)
$L + H^+ = HL^+$	6.24(1)	8.11(1)
$HL^+ + H^+ = H_2L^{2+}$	3.17(2)	6.67(2)
$H_2L^{2+} + H^+ = H_3L^{3+}$		2.51(3)

[a]Values in parentheses are the standard deviations on the last significant figure.

justified considering the higher number of protonation sites in maltonis than in malten.

Analysis of the protonation constants of maltonis starting from the anionic $H_{-2}L^{2-}$ species revealed that maltonis behaves as a strong base in the addition of the first proton (log K_1 = 11.08), and then it exhibits a quite linear decrease in the basicity with the addition of the following three protons with values ranging from 9.30 to 6.67 logarithmic units and a sharp decrease in the last proton addition (log K_5 = 2.51). This trend suggests an easy accessibility of the protonation sites up to the H_2L^{2+} species, in agreement with the ligand topology, which is prevented in the fifth step due to electrostatic repulsion. For these reasons, the four acidic protons in the H_2L^{2+} species are probably located as far as possible from each other, one on each maltol moiety and the remaining two on noncontiguous amine groups of the macrocyclic base in a disposition closely resembling that inferred from the crystal structure of this species. The values of log K_1 and log K_2 are similar to those found for the free tetraaza-macrocyclic base,[10] suggesting the involvement of the macrocyclic base in the first two protonation steps; moreover, the basicity of deprotonated free maltol[11] is similar to log K_3 and log K_4, thus supporting the involvement of the maltol functions in the third and fourth protonation steps.

Similar reasons can be invoked for malten, in which the value for the first proton addition is similar to the first protonation constant of free *N*,*N*′-dimethylethylendiamine,[12] while the second and third protonation constants are similar to the third and fourth constants of maltonis in which the involvement of the maltol functions in the protonation has been suggested. Thus, presumably, the first protonation step mainly involves the amine functions while the second and third the maltol groups of malten. In this case, the drop of the constant value was observed for the fourth proton addition (log K_4 = 3.17); taking into account that free *N*,*N*′-dimethylethylendiamine shows a higher second protonation constant (log K_2 = 7.3),[12] this lower value must be attributed not only to obviously electrostatic repulsions involving the remaining unprotonated amine function but also to a H-bonding network occurring between the close hydroxyl and these amine functions, making the latter less accessible to protonation.

The distribution of the protonated species as a function of pH is reported for both molecules in Figure 1.

UV−vis absorption electronic spectra and ^{1}H and ^{13}C NMR studies were performed in aqueous solution to investigate the distribution of protons in the various species present in solution at different pH values in depth.

UV−vis absorption electronic spectra of malten and maltonis in aqueous solutions show different features in acid or basic pH

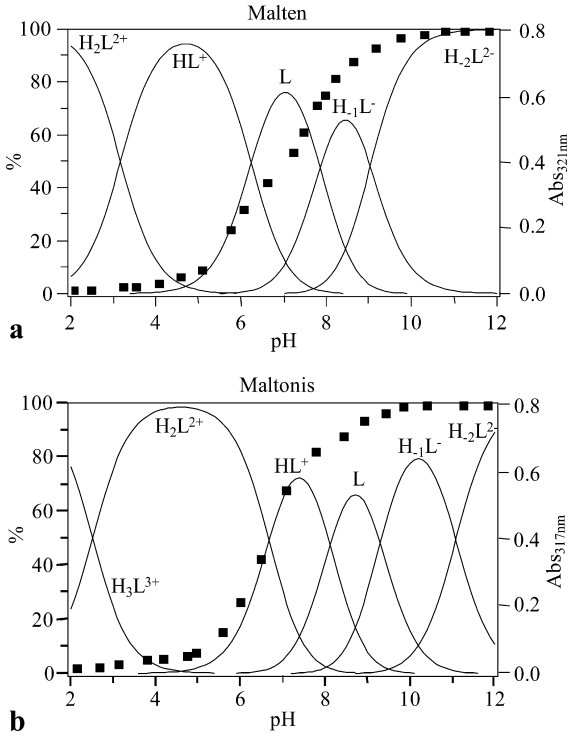

Figure 1. Distibution diagram of the species (−) and trend of the absorbance (■) for malten (a, λ = 321 nm) and maltonis (b, λ = 317 nm) in aqueous solution as a function of pH; [malten] = 3.8 × 10^{-5} M, [maltonis] = 4.0 × 10^{-5} M, I = 0.15 M NMe_4Cl, T = 298.1 K.

fields; for example, the spectrum of malten recorded at pH = 2, where the H_2L^{2+} species is prevalent in solution (see Figure 1a), exhibits a main band with λ_{max} at 275 (ε = 20200 cm^{-1} mol^{-1} dm^3). Increasing the pH, a new band with λ_{max} = 321 nm is detected, and it reaches its maximum absorbance at pH = 10 (ε = 21100 cm^{-1} mol^{-1} dm^3) while the band at higher energy disappears; no further changes were observed in the spectra at strongly alkaline pH. These different spectral features can be ascribed to the presence in solution of the neutral form of the maltol moieties at low pH values and of their deprotonated form (maltolate) at alkaline pH values. Similar reasoning can be performed for maltonis; in this case, bands with λ_{max} at 275 (ε = 22500 cm^{-1} mol^{-1} dm^3) or 317 (ε = 19600 cm^{-1} mol^{-1} dm^3) nm are shown in strong acid or basic solution, respectively.

Figure 1 reports the absorbance of the band at lower energy due to the deprotonated form of maltol together with the distribution diagram of the species as a function of pH, for malten (a) and maltonis (b), respectively.

In the case of malten, this band (λ_{max} =321 nm) appears at pH > 5.5, where the L neutral species of malten begins to exist in solution and proceeds to increase up to pH = 10 where the $H_{-1}L^-$ species is fully formed (Figure 1a).

In the case of maltonis, the same band (λ_{max} =317 nm) starts to become visible at pH > 5, where the HL^+ species of maltonis begins to be present in solution, and proceeds to increase up to pH 10 where the neutral L species is fully formed (Figure 1b). This confirms, as suggested by the potentiometric measurements, that starting from the $H_{-2}L^{2-}$ species, the amine functions are involved in the first two protonation steps for maltonis and in the first one for malten, while the maltol moieties are involved in the subsequent two steps in both molecules, i.e., L and HL^+ as well as $H_{-1}L^-$ and L for maltonis and malten, respectively.

dx.doi.org/10.1021/jo202270j | J. Org. Chem. 2012, 77, 2207−2218

In the case of maltonis, the UV−vis experiments do not allow the localization of the acidic protons on the macrocyclic base; thus, ^{1}H and ^{13}C NMR spectra were recorded over the pH range of the potentiometric experiments in order to obtain further information about the distribution of such protons. $^{1}H-^{1}H$ and $^{1}H-^{13}C$ NMR 2D correlation experiments were performed to assign all the signals. The number of ^{1}H and ^{13}C signals in the whole pH range investigated are in agreement with a C_{2v} symmetry of maltonis mediated on the NMR time-scale.

Figure 2 reports the trends for the chemical shift of the ^{1}H resonances of maltonis as a function of pH. Following the trend

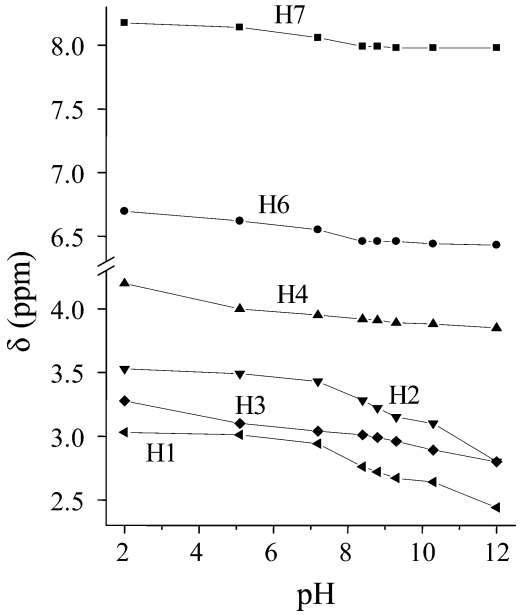

Figure 2. ^{1}H NMR chemical shifts of maltonis in aqueous solution as a function of pH.

of chemical shifts starting from pH = 12 and lowering the pH, the main shifts in the range 12−8.5, where the species $H_{-2}L^{2-}$, $H_{-1}L^{-}$, and L form, are exhibited by the methyl and methylene protons H1 and H2 (Chart 1) which show a marked downfield shift. This proves that the two protonation steps mainly involve the two methylamine functions of the macrocyclic base.

In the pH range 8−4, where the HL^{+} and H_2L^{2+} species are prevalent, the signals attributed to H6 and H7 of maltol functions shift downfield confirming that the third and fourth protonation steps occur at the maltol moieties. Obviously, the fifth protonation which leads to H_3L^{3+}, mainly giving rise to a downfield shift of the signals H3 and H4, involves the macrocyclic base and in particular the amine function bearing the maltol unit.

A protonation scheme arising from UV−vis and NMR experiments is summarized in Figure 3a for malten and in Figure 3b for maltonis.

These studies allow the determination of the active species present in the biological medium; in fact, at pH = 7.4 the main species present in solution are L and HL^{+} for malten and maltonis, respectively. In particular, the L species of malten is a zwitterion (see Figure 3a), while the HL^{+} of maltonis exhibits an internal charge separation (see Figure 3b).

In view of its overall positive charge, the latter (HL^{+} species, maltonis) could be expected to interact better than malten (L species) with the negatively charged DNA. On the other hand, solid-state and modeling data suggest that, irrespective of the overall charge and its intramolecular distribution, malten (H_2L^{2+}, L) should be more prone to act as a donor of H-bonds in intermolecular contacts than maltonis (H_2L^{2+}, HL^{+}), due to its molecular topology, which allows the ammonium groups to be generally more accessible to H-bond acceptors belonging to other species. As a consequence, malten should behave better than maltonis in a noncovalent approach with the DNA moiety. This could be the first step in the already suggested formation of covalently bound DNA structures induced by malten.[3] Within this hypothesis, we speculate that the maltol unit could behave as a Michael-type acceptor for nucleophilic sites of DNA, given that the carbon atom in 6-position (C_6, see labels for maltonis in Chart 1) bears a partial positive charge. The latter was estimated in the species of malten and maltonis present at physiological pH (L and HL^{+}, respectively) in different 3D arrangements (see the Experimental Section for details) by using the charge derivation schemes of Mullikan,[13] Merz−Singh−Kollman,[14] and natural bond orbital analysis[15] implemented in Gaussian 03, Revision C.02.[16] In all cases, the C_6 carbon atom has a partial positive charge (never less than 0.2 electrons) and the $C_6{=}C_7$ double bond is polarized, with C_7 always negatively charged.

Solid-State Studies. *$[H_2malten](ClO_4)_2{\cdot}2(H_2O)$ (**6**).* In the asymmetric unit of $[H_2malten](ClO_4)_2{\cdot}2(H_2O)$ half of the $[H_2malten]^{2+}$ cation, one perchlorate anion and one molecule of water are present.

The two halves of the cation, related by a center of symmetry, take an o_up−down conformation (see Figure 4a, Scheme 2, and MD Simulations).

Because of the presence of the center of symmetry, the rings of the maltol moieties are parallel to each other and lie on opposite sides with respect to the mean plane defined by the non-hydrogen atoms of the chain (see Figure 5a). Finally, the maltol ring mean plane forms an angle of 58.3(2)° with the mean plane containing the ethylendiamine fragment.

The crystal packing of **6** is built up by some strong hydrogen bonds[17] and $\pi-\pi$ interactions. The presence of these latter, involving two symmetry related $(-x + 1, -y + 1, -z + 2)$ maltol rings, leads to the formation of parallel chains of $[H_2malten]^{2+}$ cations (the distance between the two interacting aromatic rings is 3.37(3) Å, while the distance between the centroids of the two rings is 3.79(4) Å) (see Figures 5a and 5b). In addition, the strong hydrogen bond between the hydrogen bound to N(1) and a symmetry-related O(2) oxygen atom $(x, +y - 1, +z)$ (see Figure 5c and 4a for the atom labeling) holds together these chains, thus forming parallel sheets of $[H_2malten]^{2+}$ cations perpendicular to the *c* axis (see Figure 5d).[18] Lodged in the space between these sheets are the crystallization water molecules and the perchlorate anions. More important, hydrogen bonds (see Table 2) build up assemblies of two perchlorate anions and two water molecules $[2(ClO_4^{-})-2(H_2O)]$ which occupy the cavities present on the surface of the cation sheets (see Figure 6). Finally, because of the presence of a strong hydrogen bond involving the hydrogen linked to O(1) and one oxygen atom (O(4)) of a perchlorate anion, these $2(ClO_4^{-})-2(H_2O)$ groups link together two facing sheets.[19]

*$[H_2Maltonis](ClO_4)_2$ (**7**).* The asymmetric unit of $[H_2maltonis](ClO_4)_2$ consists of one $[H_2maltonis]^{2+}$ cation and two perchlorate anions. The macrocyclic base of the cation is in the usual [3333]C-corner conformation[20] (MD Simu-

dx.doi.org/10.1021/jo202270j | J. Org. Chem. 2012, 77, 2207−2218

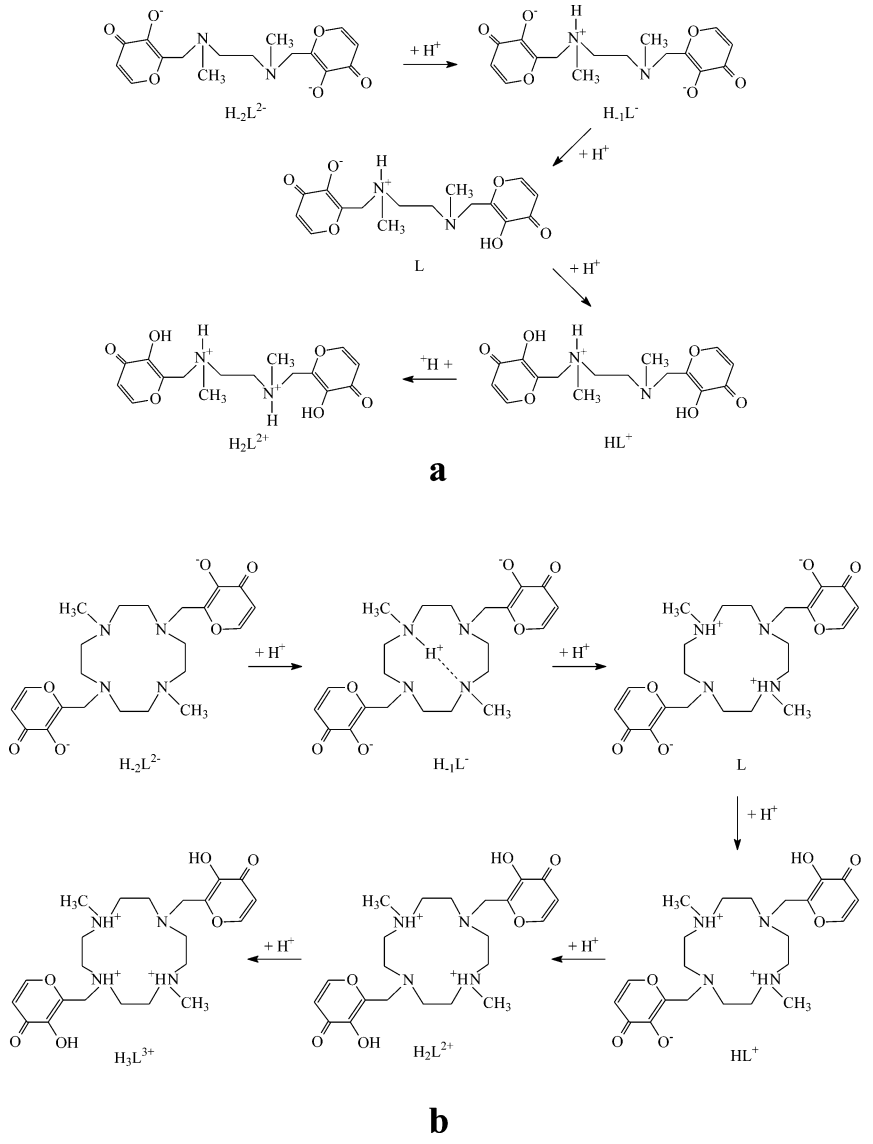

Figure 3. Location of acidic hydrogen atoms in the protonated species of malten (**a**) and maltonis (**b**).

lations), with all N···N distances comparable (about 2.9−3 Å). The acidic hydrogen atoms bound to N(1) and N(3) point inside the compound cavity and interact via weak hydrogen bonds[17] with the nitrogen atoms N(2) and N(4). The $[H_2maltonis]^{2+}$ cation interacts via a strong hydrogen bond with an oxygen atom (O13) of a perchlorate anion (see Table 2), which is above the macrocyclic cavity (Figure 7c).

The two maltol moieties lie on the same side with respect to the mean plane defined by the four nitrogen atoms of the base (see Figure 4b). Four strong intermolecular hydrogen bonds between two $[H_2maltonis]^{2+}$ cations (see Table 2 and Figure 7) give rise to the formation of a dimer. The two perchlorate anions interacting with the dimer lie on opposite sides with respect to the mean plane defined by the maltol units of the two cations (see Figure 7c).

In view of the biological test results (vide infra), it must be noted here that the $[H_2L]^{2+}$ cation is involved in the same number of intermolecular H-bond interactions in the crystal lattice of **6** and **7** (L = malten and maltonis in **6** and **7**, respectively). In fact, in both compounds, the two protonated nitrogen atoms and the oxygen of the two hydroxyl groups act as H-bonding donors while the acceptors are the oxygen atoms of the two carbonyl groups, in malten, and the oxygen atoms of a carbonyl and a hydroxyl group, in maltonis. However, the two acidic hydrogen atoms of the $[H_2maltonis]^{2+}$ cation are somehow shielded (see Figure 4b) given that they point inside the compound cavity. As a consequence, they should be less prone to interact with bulky surrounding species, as indirectly quantified by the mean distance between the opposite nitrogen atoms of the tetraaza ring (i.e., N(1)−N(3) and N(2)−N(4), 4.1 Å) and that separating the carbon atoms C(11)−C(17) and C(9)−C(10) (6.0 Å, see Figure 4b for the atom labeling), which indicates that only an acceptor atom belonging to a small group, as the perchlorate anion, can interact with these hydrogen atoms.

Modeling Studies. Molecular Dynamics (MD) simulations were performed both on the malten and maltonis H_2L^{2+} cations (see the experimental details) and on the species present at physiological pH (L and HL^+ for malten and maltonis, respectively) to gain an idea of their conformational space. As expected, a comparison between the preferred conformers obtained on the basis of an energy ground highlights how the two compounds arrange in different ways depending on their overall charge and on the nature of the surrounding medium. In

dx.doi.org/10.1021/jo202270j | J. Org. Chem. 2012, 77, 2207−2218

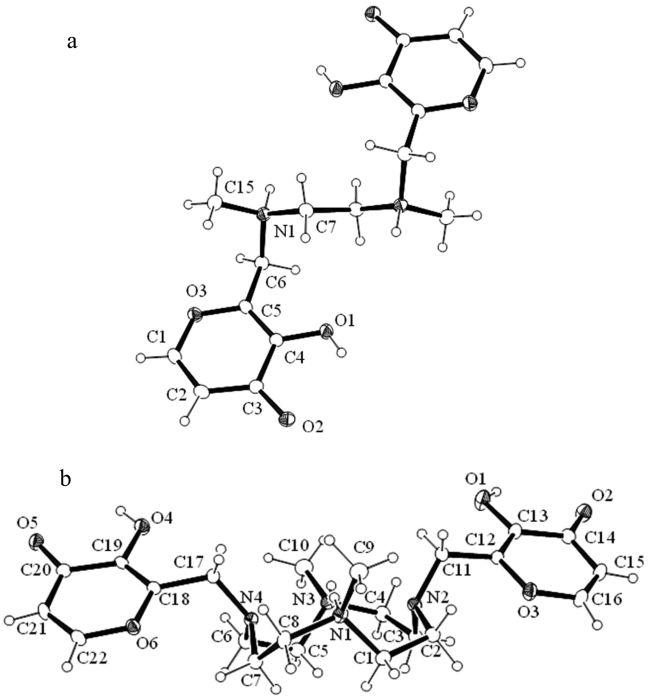

Figure 4. ORTEP3 views together with the atom labeling of $[H_2malten]^{2+}$ (a) and $[H_2maltonis]^{2+}$ (b) species. Ellipsoids are drawn at 30% probability.

Scheme 2. Orientations of Side Arms: (a) Open; (b) Face-to-Face; (c) Bent; (d) p_Up-Down; (e) o_Up-Down; (f) p–o_Up-Down

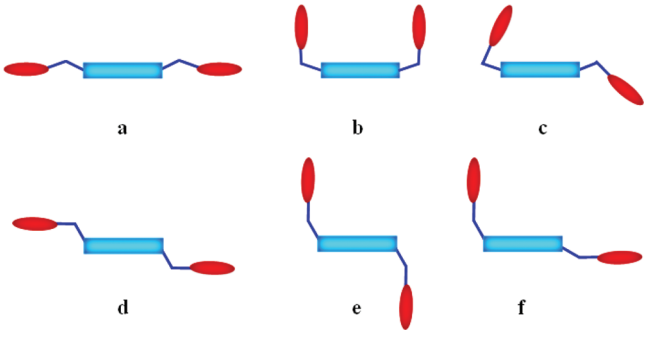

particular, we focused on the conformation adopted by the polyamine scaffold, the orientation of the two side-arms, the distances between maltol centroids, and finally on the H-bonding interactions. Five different conformations as regards the [12]aneN$_4$ macrocycle, namely the [2334]-, [3333]-, [2424]-, [13233]-, and [12333]C-corners types,[20,21] and two conformations concerning the ethylendiamine moiety, i.e., the *anti*-periplanar (NCH_2CH_2N torsion angle between 150° and 210°) and the *syn*-clinal (angle between 30° and 90°)[25] modes, were retrieved. Six side arm orientation types were found, which are illustrated in Scheme 2, and these are mainly characterized by the two side arms either both on the same side with respect to the mean plane of the polyamine framework (open (a), face-to-face (b), bent (c)) or one above and the other below the plane (parallel up–down (p_up–down, d), orthogonal up–down (o_up–down, e), or parallel-orthogonal up–down (p-o_up–down, f).

In any case, MD simulation results suggest a certain degree of flexibility, given that all of the above 3D arrangements of the

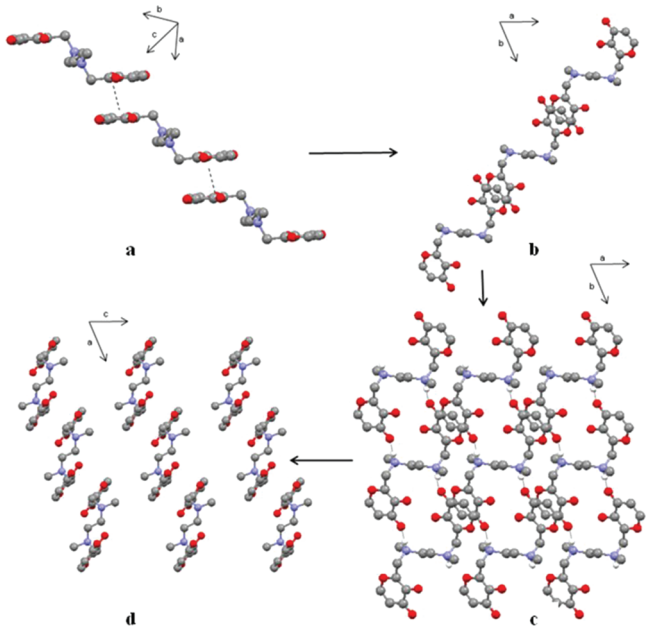

Figure 5. $[H_2malten]^{2+}$ assemblies in the crystal packing of **6**: (a and b) π–π interactions; (c) H-bond interactions viewed along the *c* axis; (d) sheets of $[H_2malten]^{2+}$ viewed along the *b* axis.

Table 2. Intermolecular Hydrogen Bonds in Compounds 6 and 7

compd	D–H···A	H···A (Å)	D–H···A (deg)
6	N(1)–H(1n)···O(2)[a]	1.73(6)	175(4)
	O(1w)–H(1w)···O(5)	2.19(3)	159(4)
	O(1w)–H(2w)···O(4)[b]	2.06(6)	147(6)
	O(1)–H(1o)···O(4)	2.07(5)	161(6)
7	N(1)–H(1n)···O(13)	2.12(2)	158(2)
	N(3)–H(3n)···O(13)	2.26(2)	154(2)
	O(4)–H(4o)···O(2)[c]	1.86(3)	155(3)
	O(1)–H(1o)···O(4)[c]	2.18(3)	165(3)

[a] $x,+y-1,+z$. [b] $-x+2,-y+2,-z+1$. [c] $-x+1,-y,-z+1$.

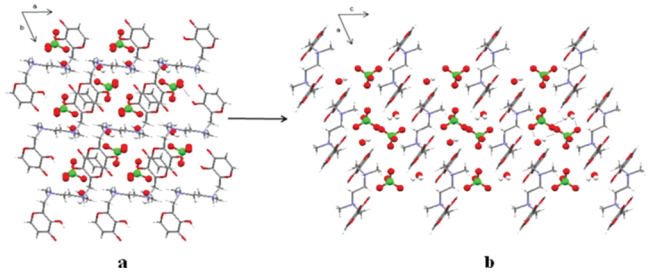

Figure 6. Crystal packing of **6**: (a and b) views along the *c* and *b* axes.

H_2L^{2+} and L/HL^+ species of the two compounds are contained in a small energy range (up to 5 kcal mol^{-1}).

Malten. *H_2L^{2+} Species.* The ethylendiamine moiety arranges itself in the *anti*-periplanar mode only in vacuo, while in most cases the *syn*-clinal mode is observed in the implicit water model, in agreement with the two positive charges to be kept apart, in the former medium, and a higher folding degree in the latter one. In vacuo, the outstretched orientation of the side arms represents 89% of the sampling, with the open arrangement (Scheme 2, Figure 8a$_i$), in particular, being the preferred one, while, as expected in polar

dx.doi.org/10.1021/jo202270j | J. Org. Chem. 2012, 77, 2207–2218

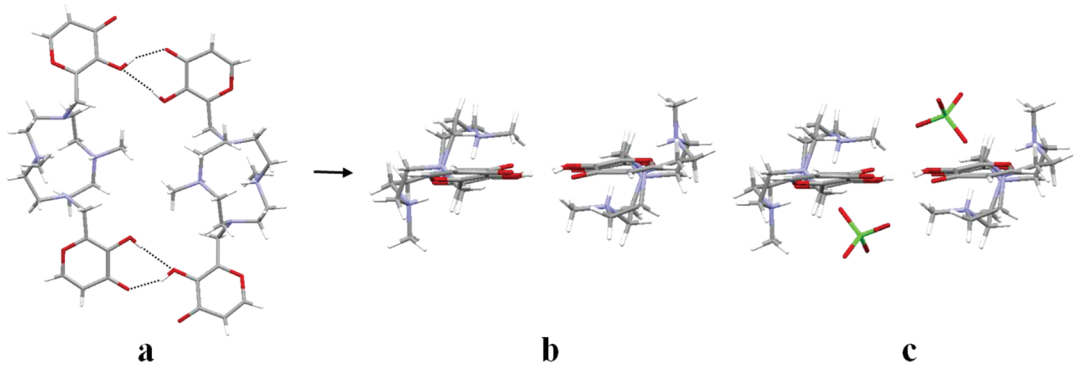

Figure 7. Crystal packing of **7**: (a) and (b) top and side views of the $[H_2maltonis]^{2+}$ dimer; (c) $[H_2maltonis]^{2+}$ dimer together with the interacting perchlorate anions.

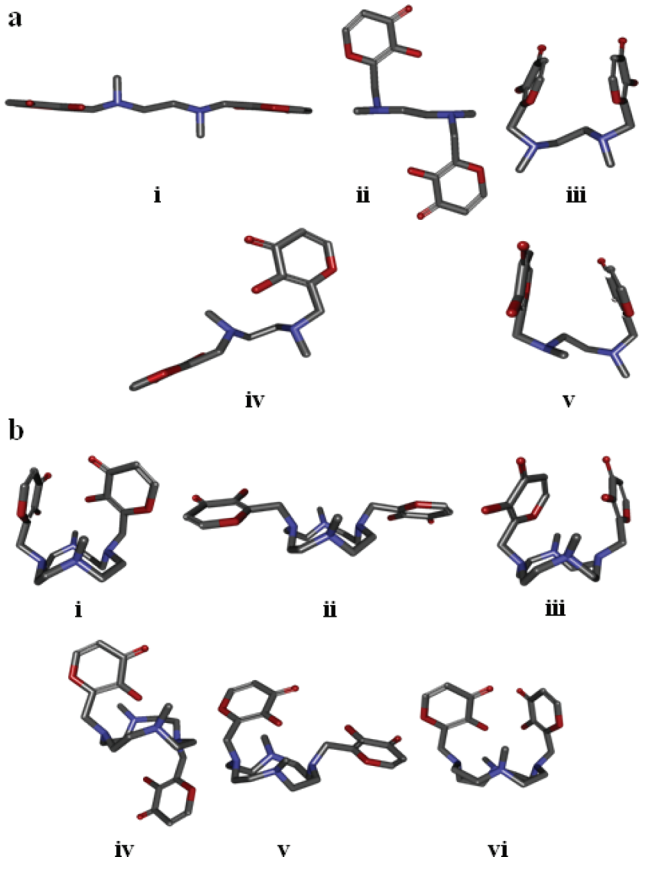

Figure 8. (a) Malten, H_2L^{2+} species: (i) *anti*-periplanar open conformation in vacuo; (ii) *anti*-periplanar o_up−down conformation in vacuo; (iii) *syn*-clinal face-to-face conformation in water. L species: (iv) *syn*-clinal p-o_up−down conformation in vacuo; (v) *syn*-clinal face-to-face conformation in water. (b) Maltonis, H_2L^{2+} species: (i) face-to-face [2334]C-corners conformation in vacuo; (ii) open [3333]C-corners conformation in vacuo; (iii) face-to-face [2334]C-corners conformation in water. HL^+ species: (iv) o_up−down [3333]C-corners conformation in vacuo; (v) bent [3333]C-corners conformation in water; (vi) face-to-face [2334]C-corners conformation in water.

solvent, the face-to-face orientation (Scheme 2, Figure $8a_{iii}$) is favored and a shortening of centroid distances is generally observed for all conformations. It is noteworthy that the o_up−down arrangement (Scheme 2, Figure $8a_{ii}$) found in vacuo is perfectly superimposable with the H_2L^{2+} cation retrieved in **6**; it lies 5 kcal mol^{-1} from the preferred face-to-face conformation, but it is the most populated family in vacuo, representing the only type which does not show intramolecular H-bondings. In fact, all of the other conformations show such interactions between each hydroxyl and the closest acidic hydrogen atom ($NH^{+}\cdots OH$), while in water most conformations do not show H-bondings, with a weakening of those still present, in agreement with the increased polarity.

L Species. Both in vacuo and in water, the *anti*-periplanar as well as the *syn*-clinal conformations are present, the latter being the most populated and the energetically preferred. The p-o_up−down and the face-to-face conformations (Scheme 2, Figure $8a_{iv}$ and $8a_{v}$) are the preferred orientations in vacuo and in water, respectively. Most conformations show intramolecular H-bondings in vacuo, with about half being between the charged oxygen and the acidic hydrogen atoms ($O^{-}\cdots HN^{+}$), as expected, while such interactions are not generally present in water.

To sum up, on moving from H_2L^{2+} to L species, the *syn*-clinal mode becomes (vacuum) or remains (water) the most populated and the distances between centroids generally shorten, in agreement with the fact that the two positive charges, in their attempt to lie as far apart as possible, are no longer present.

Finally, on moving from vacuum to water conditions, the number of side-arm orientations increases and, as expected, arrangements switch from outstretched to more folded modes. Furthermore, intramolecular H-bondings generally disappear or become weaker.

Maltonis. *H_2L^{2+} Species.* In both media, the preferred orientation of the side arms is the face-to-face one (Scheme 2, Figure $8b_{v}b_{iii}$). Although this was expected in the polar medium, in vacuo this species is likely to be strongly stabilized by multiple H-bonding interactions, making this family slightly energetically favored even if it is not the most populated one, with this being instead the outstretched open type (Scheme 2, Figure $8b_{ii}$) that is about 4 kcal mol^{-1} higher in energy and the same as retrieved in the H_2L^{2+} cation found in **7**.

HL^+ Species. As expected, in vacuo the preferred orientation of the side arms is the o_up−down (Scheme 2, Figure $8b_{iv}$), which is more outstretched than the favored families found in water, namely the bent and the face-to-face conformations (Scheme 2, Figure $8b_{v}b_{vi}$). In both media, the majority of conformations show intramolecular H-bondings, mainly between the charged oxygen of the maltolate unit and both acidic hydrogen atoms ($NH^{+}\cdots O^{-}\cdots HN^{+}$). However, in water such interactions are less numerous and weaker than in vacuo.

dx.doi.org/10.1021/jo202270j | *J. Org. Chem.* 2012, 77, 2207−2218

In summary, as expected, moving from H_2L^{2+} to HL^+ species, the number of intramolecular H-bonding interactions generally increases, especially in the vacuum model, the majority involving the charged oxygen atom, while moving from vacuum to solvent model, the conformations become more numerous and more folded. In all cases, acidic hydrogen atoms point inside the cavity of the macrocycle.

Docking Simulations. A preliminary study on the possibility for the two species of malten and maltonis present at physiological pH to interact with DNA was performed, the latter mimicked by a polynucleotide (details in the Experimental Section) at its physiological pH protonation degree. Two minimized outstretched species of L and HL^+ for malten and maltonis, respectively, were employed in the docking simulation. Both malten and maltonis are able to bridge two double-helix fragments through H-bonding and π-interactions at 300 K in vacuo and implicit water model. These results could account for the possibility for the two species to lie in a favorable position for the proposed covalent binding (see ref 3 and this work). In fact, a noncovalent approach with the DNA moiety could be the first step for the two species to place themselves in a favorable position to allow the formation of covalently bound DNA structures induced by malten,[3] whose partially positive C_6 could act as a Michael-type acceptor for nucleophilic sites of DNA, as stated above. However, malten shows a greater tendency to interact with DNA than maltonis, probably due to its flexibility which allows the maltol rings to position themselves better within the polynucleotide fragments and the ethylendiamine moiety to exhibit the acidic hydrogen atom, making it more accessible to acceptors of H-bonds than those bound to the cyclen ring of maltonis, which always point inside the cavity.

Biological Studies. *DNA–Protein Covalent Binding Induced by Malten and Maltonis.* Previous studies revealed the ability of malten to induce a complex structural alteration of genomic DNA due to the generation of DNA intermolecular cross-linking (different DNA molecules covalently bound). Herein, we further investigated - in cancer cells - the possible action of both malten and maltonis to alter the chromatin structure inducing covalent binding of genomic DNA with proteins. Promonocytic leukemia U937 cells were subjected to malten and maltonis treatments at concentrations ranging between 0.1 and 2 mM. As previously reported, malten and maltonis are able to induce a biological response in U937 cells at micromolar concentrations (IC50 values, calculated after treatments of 72 h, were 8.54 μM for malten[3] and 1.65 μM for maltonis[2]). Thus, due to the expected biological response (e.g., apoptosis), cellular treatments were performed at short exposure times (8 h) and high doses of compounds in order to limit the interference resulting from apoptosis-related DNA fragmentation. Two different assays to investigate the hypothesized action of malten and maltonis as modifiers of the chromatin structure were considered.

First, SDS/KCl precipitation assay was performed as follows: cells were treated with malten and maltonis at the concentrations reported in panel A of Figure 9, protein-bound and unbound DNA fractions were separated, and the amount (percentage) of DNA in each fraction was fluorimetrically estimated. A dose-dependent increase of DNA in protein-bound fractions was observed in cells previously treated with both malten and maltonis when compared with the amount of DNA (2.85%) estimated in the protein-bound fraction of untreated (control) cells. However, the effect induced by

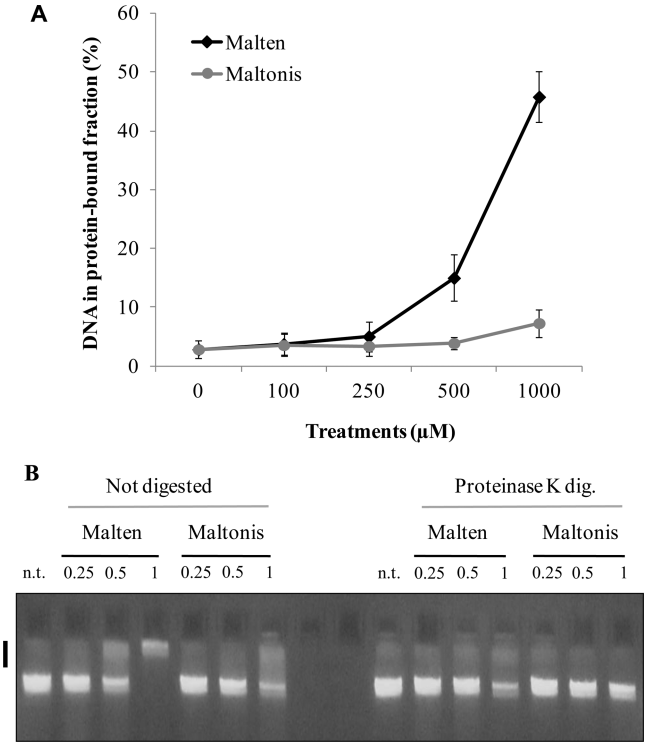

Figure 9. DNA–protein binding activity of malten and maltonis in U937 cells. (A) SDS/KCl precipitation assay. Cellular lysates obtained from U937 cells, previously treated for 8 h with different concentrations of malten (♦) or maltonis (●), were fractioned by SDS/KCl precipitation and the amount of DNA fluorimetrically quantified. (B) Impaired electrophoretic mobility of genomic DNA. Genomic DNA, extracted from U937 cells treated or not treated (n.t.) for 8 h with the reported concentrations of malten or maltonis, were incubated in 2% SDS solution, digested or not digested with 200 μg/mL proteinase K and separated by agarose gel electrophoresis (AGE). (Black bar) genomic DNA with impared electophoretic mobility.

malten and maltonis is quite different: up to 45% of DNA can be monitored in the protein-bound fraction of cells incubated with malten at the concentration of 1 mM, while only 7.3% of DNA can be estimated at the same concentration of maltonis.

The DNA–protein binding activity of malten and maltonis was then further investigated in U937 cells through a canonical agarose gel electrophoretic assay. As shown in panel B of Figure 9, we demonstrated that both molecules impair the electrophoretic migration of SDS-extracted genomic DNA. In accordance with the previous assay, we found that malten induces a significant effect starting from the concentration of 0.5 mM, while maltonis activity is detectable only at the dose of 1 mM. In order to establish if the impaired electrophoretic migration was ascribable to the binding of genomic DNA with proteins, samples were subjected to protein digestion with proteinase K. Interestingly, we found that proteinase K treatment totally reverses this effect, indicating that the binding of DNA with proteins was mainly responsible for the impaired electrophoretic migration of genomic DNA. Interestingly, CDDP (or cisplatin), a compound largely used as chemotherapeutic agent, is known to act prevalently modifying DNA through the generation of intrastrand and interstrand molecular cross-linking (covalent modification that takes place in the same DNA molecule), but it is not able to generate intermolecular cross-linking. Recently, the ability of CDDP to form DNA–protein cross-links in a cell-free assay has been

dx.doi.org/10.1021/jo202270j | J. Org. Chem. 2012, 77, 2207–2218

proven.[26] Furthermore, a novel trans-platinum compound (ATZ) demonstrates antiproliferative and cytotoxic effects against cancer cells reconducible to its ability to induce DNA covalent modifications and DNA breaks. The authors demonstrated also that AZT was able to generate DNA–protein cross-linking by a similar experimental procedure (SDS/KCl precipitation assay) using a short exposure time (12 h) and with the necessity to increase the concentration of the drug in the cellular treatments in order to avoid interference with the precipitation assay itself.[27]

Taken together, these observations demonstrate that both molecules are able to induce the binding of cellular proteins with genomic DNA, thus suggesting the ability of malten (and to a lesser extent of maltonis) to alter the chromatin structure.

CONCLUSIONS

The *N,N′*-bis[(3-hydroxy-4-pyron-2-yl)methyl]-*N,N′*-dimethylethylendiamine (malten) and 4,10-bis[(3-hydroxy-4-pyron-2-yl)methyl]-1,7-dimethyl-1,4,7,10-tetraazacyclododecane (maltonis) were synthesized and characterized; the synthetic procedure allows the attainment of both molecules as hydroperchlorate salts in good yields.

The neutral species of both molecules behaves as a diprotic acid while it behaves as a diprotic or triprotic base for malten and maltonis, respectively, in aqueous solution under the experimental conditions used. The NMR and UV–vis experiments allowed the determination of the disposition of the acidic protons occurring in the several species present at different pH values; in particular, at pH 7.4 the main species present in solution are L and HL^+ for malten and maltonis, respectively. The L species of malten, showing one deprotonated maltol unit and one protonated amine group, is in a zwitterionic form; the HL^+ species of maltonis exhibits an internal separation of the charges with the presence of two ammonium groups and a deprotonated maltol unit.

Solid-state results reveal that although the $[H_2L]^{2+}$ cations are involved in the same number of intermolecular H-bonds, the two acidic hydrogen atoms of the $[H_2maltonis]^{2+}$ cation, which point inside the compound cavity, are undoubtedly shielded and thus less accessible to bulky surrounding species. In addition, MD simulations in water mimicked medium on the [malten] species show a large variety of different conformations of side-arms and a small tendency to form intramolecular H-bondings. In the same simulation conditions, the $[Hmaltonis]^+$ cation can also access numerous different conformations; however, the acidic hydrogen atoms always point inside the cavity of the cation and the intramolecolar network of H-bonds is maintained. Thus, on the basis of these results, we can hypothesize a different biological activity/efficiency of malten with respect to maltonis: the molecular topology of the open compound should be favored in the H-bond mediated interaction with the DNA moiety, as suggested by the docking simulations. In support of this hypothesis, malten was more efficient than maltonis in inducing the chromatin modifications (Figure 9).

The novel observation shown in this study regarding the ability to induce covalent binding between DNA and proteins, together with the previous reported property of malten to cause complex structural alteration of genomic DNA,[3] strongly supports the hypothesis of an interference with the chromatin structure as part of the molecular mechanisms responsible for the biological activity exerted by this group of molecules against cancer cells.

EXPERIMENTAL SECTION

General Methods. UV/vis absorption spectra were recorded at 298 K on a spectrophotometer equipped with a temperature control unit. ^1H and ^{13}C NMR spectra were recorded on an instrument, operating at 200.13 and 50.33 MHz, respectively, and equipped with a variable-temperature controller. The temperature of the NMR probe was calibrated using 1,2-ethanediol as calibration sample. For the spectra recorded in D_2O, the peak positions are reported with respect to HOD (4.75 ppm) for ^1H NMR spectra, while dioxane was used as reference standard in ^{13}C NMR spectra (δ = 67.4 ppm). For the spectra recorded in $CDCl_3$ the peak positions are reported with respect to TMS. $^1H-^1H$ and $^1H-^{13}C$ correlation experiments were performed to assign the signals.

Synthesis. Compounds malten and maltonis were obtained following the synthetic procedure reported in Scheme 1. 1,7-Dimethyl-1,4,7,10-tetraazacyclododecane (**5**)[9] was prepared as previously described. All other chemicals were purchased in the highest quality commercially available. The solvents were RP grade, unless otherwise indicated.

*3-(tert-Butyldimethylsilyl)oxy-2-methyl-4-pyrone (**2**).* A solution of imidazole (Im, 5.45 g, 0.08 mol) in *N,N*-dimethylformamide (20 mL) was added in an inert atmosphere and dropwise to a solution containing 3-hydroxy-2-methyl-4-pyrone (**1**) (5.00 g, 0.04 mol) and *tert*-butyldimethylchlorosilane (TBDMSCl, 7.00 g, 0.044 mol) in *N,N*-dimethylformamide (100 mL). The mixture obtained was maintained under stirring at a room temperature for 6 h and then diluted by addition of a 5% hydrogen carbonate aqueous solution (150 mL). The mixture obtained was extracted with hexane (6 × 50 mL); the extracted organic phases were combined, dried on sodium sulfate, and evaporated under vacuum to obtain the 3-(*tert*-butyldimethylsilyl)oxy-2-methyl-4-pyrone (**2**) as a colorless crystalline solid (9.61 g, 98%): ^1H NMR ($CDCl_3$, 25 °C) 7.58 (d, 1H, J = 5.56 Hz), 6.29 (d, 1H, J = 5.56 Hz), 2.31 (s, 3H), 0.96 (s, 9H), 0.26 (s, 6H); ^{13}C NMR ($CDCl_3$, 25 °C) 174.0, 154.6, 152.8, 142.8, 115.5, 25.9, 18.7, 14.8, 3.8.

N,N′-Bis[(3-hydroxy-4-pyron-2-yl)methyl]-N,N′-dimethylethylendiamine Dihydroperchlorate (Malten·2HClO$_4$). α,α′-Azoisobutyrronitrile (AIBN, 0.33 g, 0.002 mol) was added under an inert atmosphere to a refluxing and stirred solution of **2** (3.5 g, 0.015 mol) and *N*-bromosuccinimide (NBS, 3.0 g, 0.016 mol) in CCl_4 (70 mL). The resulting mixture was maintained by stirring and with reflux for 1 h and testing with TLC on silica gel (hexane/ethyl acetate 1:1 eluent; R_f = 0.85); the mixture was subsequently cooled at room temperature and then filtered. The resulting yellow solution containing compound **3** was used without further purification by adding it dropwise in an inert atmosphere at 0 °C to a solution of *N,N′*-dimethylethylendiamine (**4**, 0.45 g, 0.005 mol) and triethylamine (TEA, 2.12 mL, 0.015 mol) in THF (70 mL). The reaction mixture was maintained by stirring at 0 °C for 48 h and then filtered, resulting in a red-orange solution which was coevaporated under vacuum several times with ethanol (3 × 100 mL). The resulting red oil residue was dissolved in ethanol (50 mL), and 10% perchloric acid solution was added dropwise to the resulting solution until total precipitation of a yellow solid. The solid was filtered, washed with ethanol, and recrystallized using sodium perchlorate saturated water to obtain malten·2HClO$_4$ as a white solid (1.67 g, 58%): ^1H NMR (D_2O pH = 2, 25 °C) 7.97 (d, 2H, J = 5.55 Hz), 6.43 (d, 2H, J = 5.55 Hz), 4.43 (s, 4H), 3.62 (s, 4H), 2.87 (s, 6H); ^{13}C NMR (D_2O pH = 2, 25 °C) 175.3, 157.2, 147.0, 140.1, 114.0, 52.1, 49.1, 40.9; MS (m/z) 337.3 (M + H). Anal. Calcd for $C_{16}H_{22}Cl_2N_2O_{14}$: C, 32.76; H, 4.32; N, 5.46. Found: C, 32.8; H, 4.3; N, 5.5.

*[H$_2$Malten](ClO$_4$)$_2$·2(H$_2$O) (**6**).* Colorless crystals suitable for X-ray analysis were obtained by slow evaporation of malten·2HClO$_4$ (53.7 mg, 0.1 mmol) dissolved in H_2O (10 mL) and adjusting the pH to 2 with $HClO_4$ 0.1 M. Anal. Calcd for $[H_2malten](ClO_4)_2(H_2O)$ (**6**) $C_{16}H_{24}Cl_2N_2O_{15}$: C, 34.61; H, 4.36; N, 5.04. Found: C, 34.6; H, 4.3; N, 5.1.

4,10-Bis[(3-hydroxy-4-pyron-2-yl)methyl]-1,7-dimethyl-1,4,7,10-tetraazacyclododecane Tetrahydroperchlorate (Maltonis·3HClO$_4$·H$_2$O). Compound **3** was prepared as previously disclosed from α,α′-azoisobutyronitrile (AIBN, 0.33 g, 0.002 mol), **2** (3.5 g, 0.015

dx.doi.org/10.1021/jo202270j | J. Org. Chem. 2012, 77, 2207–2218

mol), and *N*-bromosuccinimide (NBS, 3.0 g, 0.016 mol) in carbon tetrachloride and used immediately without further purification. Compound **3** was added at 0 °C dropwise in an inert atmosphere to a solution of 1,7-dimethyl-1,4,7,10-tetraazacyclododecane (**5**, 1.00 g, 0.005 mol) and triethylamine (TEA, 2.12 mL, 0.015 mol) in THF (70 mL). The reaction mixture was maintained by stirring at 0 °C for 12 h and then coevaporated under vacuum with ethanol (3 × 100 mL). The resulting residue was a red oil which was solubilized in ethanol (50 mL); 10% perchloric acid solution in ethanol was added dropwise to the resulting solution until total precipitation of a white solid which was filtered, washed with ethanol, and recrystallized by sodium perchlorate saturated water obtaining maltonis·3$HClO_4$·H_2O as a white solid (1.69 g, 44%): ^{1}H NMR (D_2O pH = 2, 25 °C) 7.99 (d, 2H, J = 5.50 Hz), 6.46 (d, 2H, J = 5.50 Hz), 3.89 (s, 4H), 3.36 (m, 8H), 2.96 (m, 8H), 2.88 (s, 6H); ^{13}C NMR (D_2O pH = 2, 25 °C) 175.4, 157.1, 149.8, 144.7, 114.0, 53.4, 49.0, 47.2, 42.4; MS (m/z) 449.5 (M + H). Anal. Calcd for $C_{22}H_{37}Cl_3N_4O_{19}$: C, 34.41; H, 4.86; N, 7.30. Found: C, 34.4; H, 4.8; N, 7.4.

*[H_2Maltonis](ClO_4)$_2$ (**7**).* Maltonis·3$HClO_4$·H_2O (38.4 mg, 0.05 mmol) was dissolved in H_2O (10 mL), $NaClO_4$ (61 mg, 0.5 mmol) was added to the solution, and the pH was adjusted to 4.5 with NaOH 0.1 M. Colorless crystals suitable for X-ray analysis formed in 1 day at room temperature (23 mg, 71%). Anal. Calcd for [H_2maltonis](ClO_4)$_2$ (**7**) $C_{22}H_{34}Cl_2N_4O_{14}$: C, 40.69; H, 5.28; N, 8.63. Found: C, 40.6; H,5.3; N, 8.6.

Caution. *Perchlorate salts of organic compounds are potentially explosive; these compounds must be prepared and handled with care!*

EMF Measurements. Equilibrium constants for protonation reactions with malten and maltonis were determined by pH-metric measurements (pH = −log [H^+]) in 0.15 M NMe_4Cl at 298.1 ± 0.1 K, using the fully automatic equipment that has already been described;[28] the EMF data were acquired with the PASAT computer program.[29] The combined glass electrode was calibrated as a hydrogen concentration probe by titrating known amounts of $HClO_4$ with CO_2-free NMe_4OH solutions and determining the equivalent point by Gran's method,[30] which gives the standard potential $E°$ and the ionic product of water (pK_w = 13.83(1), K_w = [H^+][OH^-]). At least three potentiometric titrations were performed for each system in the pH range 2−11. All titrations were treated either as single sets or as separate entities, for each system; no significant variations were found in the values of the determined constants. The HYPERQUAD computer program was used to process the potentiometric data.[31]

Cell Cultures and Treatments. Immortalized promonocytic leukemia U937 cells were obtained from the American Type Culture Collection (ATTC, Rockville, MD). Cells were grown in RPMI 1640 (Cambrex, Walkersville, MD) supplemented with 10% fetal bovine serum, 1% penicillin−streptomycin, and 1% glutamine under conditions as previously described.[32]

Malten and maltonis were dissolved, respectively, at 25 and 12 mM in double-distilled water as stock solution, stored at −80 °C, and subsequently diluted just before use. Treatments were performed for 8 h at the concentrations reported in the figures.

SDS/KCl Precipitation Assay. SDS/KCl assays were conducted as described.[33] DNA−protein cross-link formation in rat nasal epithelial cells by hexamethylphosphoramide and its correlation with formaldehyde production (mutation res 343:209-218) were studied. Briefly, after incubation with malten or maltonis, U937 cells were harvested, washed with ice-cold 1× PBS, and resuspended in 1× PBS, 2.5% SDS. DNA was shared by pipetting, and KCl was added at the final concentration of 175 mM. After incubation on ice for 5 min, precipitated proteins and DNA−protein complexes were pelletted by centrifugation at 13400*g* for 5 min (at 4 °C), and supernatants, containing the unbound fractions of DNA, were collected. Pellets were washed two times in ice-cold 0.1 M KCl, 0.1 mM EDTA, 10 mM Tris-HCl (pH 7.4); each wash step was followed by 5 min of incubation on ice and centrifugation at 13400*g* for 5 min (at 4 °C). Supernatants, obtained from each wash step, were pooled with previous unbound DNA fractions. Then pellets were resuspended in 1 mL of 0.1 M KCl, 10 mM EDTA, and 40 mM Tris−HCl (pH 6.5) and digested with 200 μg/mL proteinase K for 3 h at 45 °C. After further incubation on ice for 5 min, samples were centrifuged at 13400*g* for 5 min (at 4 °C) and supernatants containing the bound fraction of DNA were collected. Finally, DNA contents of both bound and unbound fractions were fluorimetrically quantified by Qubit (Invitrogen, Carlsbad, CA).

DNA Electrophoretic Mobility Assay. U937 cells untreated (control), or treated with malten or maltonis, were harvested, washed once with ice-cold 1× PBS, resuspended in a solution containing 1× PBS, 2% SDS, 10 μg/mL RNase A at the concentration of 10^6 cells/mL, and incubated overnight at 4 °C.[3] Subsequently, each sample was divided into two aliquots: the first aliquot was digested with 200 μg/mL proteinase K for 3 h at 45 °C, while the second was incubated 3 h at 45 °C in the absence of proteinase K. Genomic DNA was then separated by 1% agarose gel electrophoresis (AGE) and detected by ethidium bromide staining.

X-ray Crystallography. Intensity data for compounds [H_2malten](ClO_4)$_2$·(H_2O) (**6**) and [H_2maltonis](ClO_4)$_2$ (**7**) were collected on a diffractometer using Mo Kα radiation (λ = 0.71069 Å). Data collection was performed with the program CrysAlis CCD;[34] data reduction for the two structures was carried out with the program CrysAlis RED;[35] absorption correction was performed with the program ABSPACK in CrysAlis RED.[36]

The structures of **6** and **7** were solved by using the SIR-97 package[37] and subsequently refined on the F^2 values by the full-matrix least-squares program SHELXL-97.[38]

All of the non-hydrogen atoms of the two structures were anisotropically refined, while all the hydrogen atoms were found via Fourier synthesis and refined isotropically.

Geometrical calculations were performed by PARST97,[39] and molecular plots were produced by the Mercury 2.4[40] and ORTEP3[41] programs.

Crystallographic data and refinement parameters are reported in the Supporting Information (Table S1).

Computational Details. The Gaussian03 (Revision C.02)[16] package implemented on a personal computer was used. In all cases, the level of theory was HF-SCF, the basis set was 6-311G(d,p),[42] and the Berny algorithm was used.[43] The input geometries for the L and HL^+ species of malten and maltonis, respectively, were chosen among those found in the MD simulations.

Molecular Simulations. Geometric optimizations (MM) and molecular dynamics (MD) simulations were performed on the H_2L^{2+} cations found in the two X-ray crystal structures **6** and **7** and on the L and HL^+ species (for malten and maltonis, respectively), derived from the parent compound. The starting geometries of all the species employed in the MD simulations were obtained minimizing the H_2L^{2+} conformations retrieved in **6** and **7**. MD simulations were carried out at 300, 600, and 900 K, both in vacuo as well as in an implicit water model; water calculations were performed mimicking the solvent by using a distance-dependent dielectric constant of 80.0. All calculations were made by using the CHARMm[44] force field. MM calculations were performed on each species by using the Smart Minimizer energy minimization procedure implemented in Accelrys Discovery Studio 2.1[45] and before starting the MD simulations, the geometry of each compound was further optimized using the steepest descent, conjugate gradient and finally Newton−Raphson algorithms. In the molecular dynamics, the time step was 1 fs for all runs, while equilibration times ranged from 100 to 8000 ps and production times from 1000 to 100000 ps, depending on the charge and the surrounding medium. The programs used for the MD and the energy minimization were the simulation protocols Standard Dynamics Cascade and Minimization implemented in Discovery Studio. The starting geometry for the polynucleotide 5′-D(*CP*AP*CP*GP*TP*G)-3′[46] was retrieved from the RCSB Protein Bank Database. Docking simulations were performed at 300 K both in vacuo and in the simulated water solvent by using the same protocol Standard Dynamics Cascade implemented in Discovery Studio.

■ ASSOCIATED CONTENT

Supporting Information

Crystallographic data (CIF) for compounds **6** and **7**. Table S1 containing crystallographic data and refinement parameters for compounds **6** and **7**; ^{1}H and ^{13}C NMR spectra of malten and maltonis compounds. This material is available free of charge via the Internet at http://pubs.acs.org.

■ AUTHOR INFORMATION

Corresponding Author

*E-mail: (V.F) vieri.fusi@uniurb.it, (M.F.) mirco.fanelli@uniurb.it, (P.P.) paolapaoli@unifi.it.

Notes

The authors declare no competing financial interest.

■ ACKNOWLEDGMENTS

We thank the Italian Ministero dell'Istruzione dell'Università e della Ricerca (MIUR), PRIN2008 and PRIN2009, and the Associazione a Sostegno degli Studi Oncologici (ASSO) for financial support. X-ray data collection was performed at CRIST (Centro di Crystallografia Strutturale), University of Florence.

■ REFERENCES

(1) Hochhauser, T.; Tobias, J. *Cancer and Its Management*, 6th ed.; Wiley-Blackwell, Oxford, 2010.

(2) Fanelli, M.; Fusi, V. PCT Int. Appl. WO 2010061282 A1 20100603, 2010.

(3) Amatori, S.; Bagaloni, I.; Fanelli, M.; Formica, M.; Fusi, V.; Giorgi, L.; Macedi, E. *Brit. J. Cancer.* **2010**, *103*, 239−248.

(4) (a) Gralla, E. J.; Stebins, R. B.; Coleman, G. L.; Delahunt, C. S. *Toxicol. Appl. Pharmacol.* **1969**, *15*, 604−613. (b) Bjeldanes, L. F.; Chew, H. *Mutat. Res.* **1969**, *67*, 367−371.

(5) (a) Hironishi, M.; Kordek, R.; Yanagihara, R.; Garruto, R. M. *Neurodegeneration* **1996**, *5*, 325−329. (b) Yasumoto, E.; Nakano, K.; Nakayachi, T.; Morshed, S. R.; Hashimoto, K.; Kikuchi, H.; Nishikawa, H.; Kawase, M.; Sakagami, H. *Anticancer Res.* **2004**, *24*, 755−762. (c) Murakami, K.; Ishida, K.; Watakabe, K.; Tsubouchi, R.; Haneda, M.; Yoshino, M. *Biometals* **2006**, *19*, 253−257. (d) Murakami, K.; Ishida, K.; Watakabe, K.; Tsubouchi, R.; Naruse, M.; Yoshino, M. *Toxicol. Lett.* **2006**, *161*, 102−107.

(6) (a) Bransovà, J.; Brtko, J.; Uher, M.; Novotny, L. *Int. J. Cell. Biol.* **1995**, *7*, 701−706. (b) Jakupec, M. A.; Keppler, B. K. *Curr. Top. Med..Chem.* **2004**, *4*, 1575−1583. (c) Barve, A.; Kumbhar, A.; Bhat, M.; Joshi, B.; Butcher, R.; Sonawane, U.; Joshi, R. *Inorg. Chem.* **2009**, *48*, 9120−9132. (d) Kandioller, W.; Hartinger, C. G.; Nazarov, A. A.; Kasser, J.; John, R.; Jakupec, M. A.; Arion, V. B.; Dyson, P. J.; Keppler, B. K. *J. Organomet. Chem.* **2009**, *694*, 922−929. (e) Song, B.; Saatchi, K.; Rawji, G. H.; Orvig, C. *Inorg. Chim. Acta* **2002**, *339*, 393−399. (f) Saatchi, K.; Thompson, K. H.; Patrick, B. O.; Pink, M.; Yuen, V. G.; McNeill, J. H.; Orvig, C. *Inorg.c Chem.* **2005**, *44* (8), 2689−2697.

(7) (a) Liang, F.; Wan, S.; Li, Z.; Xiong, X.; Yang, L.; Zhou, X.; Wu, C. *Curr. Med. Chem.* **2006**, *13*, 711−727. (b) Casero, R. A. J.; Woster, P. M. *J. Med. Chem.* **2001**, *44*, 1−26. (c) Parker, D.; Millican, T. A.; Beeley, N. R. A. *Eur. Pat. Appl.* EP 382583 A1 19900816, 1990.

(8) (a) Kendall, P. M.; Johnson, J. V.; Cook, C. E. *J. Org. Chem.* **1979**, *44*, 1421−1424. (b) Rodríguez, J. R.; Rumbo, A.; Castedo, L.; Mascarenas, J. L. *J. Org. Chem.* **1999**, *64*, 966−970.

(9) Fusi, V.; Giorgi, L.; Piersanti, G.; Varrese, M. A.; Zappia, G. *Tetrahedron Lett.* **2010**, *51*, 3436−3438.

(10) Ciampolini, M.; Dapporto, P.; Micheloni, M.; Nardi, N.; Paoletti, P.; Zanobini, F. *J. Chem. Soc., Dalton Trans.* **1984**, 1357.

(11) Elvingson, E.; Baro, L.; Petterson, L. *Inorg. Chem.* **1996**, *35*, 3388.

(12) Barbucci, R.; Fabbrizzi, L.; Paoletti, P. *J. Chem. Soc., Dalton Trans.* **1972**, 745−749.

(13) Mullikan, R. S. *J. Chem. Phys.* **1955**, *23*, 1833−1840, 1841−1846, 2338−2342, 2343−2346.

(14) (a) Singh, U. C.; Kollman, P. A. *J. Comput. Chem.* **1984**, *5*, 129. (b) Besler, B. H.; Merz, K. M. J..; Kollman, P. A. *J. Comput. Chem.* **1990**, *11*, 431.

(15) (a) Carpenter, J. E.; Weinhold, F. *THEOCHEM* **1988**, *169*, 41. (b) Reed, A. E.; Curtiss, L. A.; Weinhold, F. *Chem. Rev.* **1988**, *88*, 899 and references therein.

(16) Gaussian 03, Revision C.02. Frisch, M. J.; Trucks, G. W.; Schlegel, H. B.; Scuseria, G. E.; Robb, M. A.; Cheeseman, J. R.; Montgomery, J. A., Jr.; Vreven, T.; Kudin, K. N.; Burant, J. C.; Millam, J. M.; Iyengar, S. S.; Tomasi, J.; Barone, V.; Mennucci, B.; Cossi, M.; Scalmani, G.; Rega, N.: Petersson, G. A.; Nakatsuji, H.; Hada, M.; Ehara, M.; Toyota, K.; Fukuda, R.; Hasegawa, J.; Ishida, M.; Nakajima, T.; Honda, Y.; Kitao, O.; Nakai, H.; Klene, M.; Li, X.; Knox, J. E.; Hratchian, H. P.; Cross, J. B.; Adamo, C.; Jaramillo, J.; Gomperts, R.; Stratmann, R. E.; Yazyev, O.; Austin, A. J.; Cammi, R.; Pomelli, C.; Ochterski, J. W.; Ayala, P. Y.; Morokuma, K.; Voth, G. A.; Salvador, P.; Dannenberg, J. J.; Zakrzewski, V. G.; Dapprich, S.; Daniels, A. D.; Strain, M. C.; Farkas, O.; Malick, D. K.; Rabuck, A. D.; Raghavachari, K.; Foresman, J. B.; Ortiz, J. V.; Cui, Q.; Baboul, A. G.; Clifford, S.; Cioslowski, J.; Stefanov, B. B.; Liu, G.; Liashenko, A.; Piskorz, P.; Komaromi, I.; Martin, R. L.; Fox, D. J.; Keith, T.; Al-Laham, M. A.; Peng, C. Y.; Nanayakkara, A.; Challacombe, M.; Gill, P. M. W.; Johnson, B.; Chen, W.; Wong, M. W.; Gonzalez, C.; Pople, J. A. Gaussian, Inc., Wallingford, CT, 2004.

(17) Desiraju, G. R.; Steiner, T. The weak hydrogen bond. *IUCr Monographs on Crystallography*; Oxford Science Publications: Oxford, 1999.

(18) The tendency of the $[H_2malten]^{2+}$ cation to form this type of parallel sheets is proved by the very similar crystal packing shown by the $[H_2malten](PtCl_4)_2(H_2O)$ compound (unpublished results).

(19) An ethylenediamine derivative (CSD refcode LEZPEM: Solis, E. O.; de Barbarin, C. R.; de Cota, P. E.; Martinez, B. N. *Ciencia UANL* **2001**, *4*, 435−440) with a crystal packing very similar to the one studied in this work was retrieved in the Cambridge Structural Database (CSD, v 5.32). In that case, too, the crystallization water molecules are linked by hydrogen bonds to the counterions (chloride anions in the LEZPEM case), thus forming $2(Cl^-)-2(H_2O)$ groups that occupy the space between parallel sheets of $(H_2L)^{2+}$ cations (L = *N*,*N*′-bis(2-nitrobenzyl)-1,2-diaminoethane

(20) Bernal, I., Ed. *Stereochemical and Stereophysical Behaviour of Macrocycles*; Elsevier: Amsterdam, 1987; p 34.

(21) The [2334]C-corners conformation is unusual to define the diprotonated cyclen ring, according to the analysis of the solid-state structures collected in the Cambridge Structural Database, which revealed that among the 27 results found the majority adopts the square [3333]C-corners conformation[22] (which we found in the $(H_2L)^{2+}$ cation of **7**) with three exceptions of the [2424]C-corners[22b,23] and two of the [2334]C-corners types.[22i,24]

(22) (a) Kobayashi, K.; Tsuboyama, S.; Tsuboyama, K.; Sakurai, T. *Acta Crystallogr., Sect. C: Cryst. Struct. Commun.* **1994**, *50*, 306. (b) Bencini, A.; Bianchi, A.; Bazzicalupi, C.; Ciampolini, M.; Dapporto, P.; Fusi, V.; Micheloni, M.; Nardi, N.; Paoli, P.; Valtancoli, B. *J. Chem. Soc., Perkin Trans. 2* **1993**, 115. (c) Aime, S.; Batsanov, A S.; Botta, M.; Howard, J. A. K.; Parker, D.; Senanayake, K.; Williams, G. *Inorg. Chem.* **1994**, *33*, 4696. (d) Bazzicalupi, C.; Bencini, A.; Bianchi, A.; Fusi, V.; Paoletti, P.; Valtancoli, B. *J. Chem. Soc., Perkin Trans. 2* **1994**, 815. (e) Bianchi, A.; Ciampolini, M.; Micheloni, M.; Nardi, N.; Valtancoli, B.; Mangani, S.; Garcia-Espana, E.; Ramirez, J. A. *J. Chem. Soc., Perkin Trans. 2* **1989**, 1131. (f) Vitha, T.; Kubíček, V.; Kotek, J.; Hermann, P.; Vander Elst, L.; Muller, R. N.; Lukeš, I.; Peters, J. A. *Dalton Trans.* **2009**, 3204. (g) Ambrosi, G.; Dapporto, P.; Formica, M.; Fusi, V.; Giorgi, L.; Guerri, A.; Lucarini, S.; Micheloni, M.; Paoli, P.; Pontellini, R.; Rossi, P.; Zappia, G. *New J. Chem.* **2004**, *28*, 1359. (h) Aime, S.; Barge, A.; Bruce, J. I.; Botta, M.; Howard, J. A. K.; Moloney, J. M.; Parker, D.; de Sousa, A. S.; Woods, M. *J. Am. Chem. Soc.* **1999**, *121*, 5762. (i) Micheloni, M.; Formica, M.; Fusi, V.; Romani, P.; Pontellini, R; Dapporto, P.; Paoli, P.; Rossi, P.; Valtancoli, B- *Eur. J. Inorg. Chem.*

2000, 51. (j) Woods, M.; Aime, S.; Botta, M.; Howard, J. A. K.; Moloney, J. M.; Navet, M.; Parker, D.; Port, M.; Rousseaux, O. *J. Am. Chem. Soc.* **2000**, *122*, 9781. (k) Försterová, M.; Svobodová, I.; Lubal, P.; Táborský, P.; Kotek, J.; Hermann, P.; Lukeš, I. *Dalton Trans.* **2007**, 535. (l) Polášek, M.; Sedinová, M.; Kotek, J.; Vander Elst, L.; Muller, R. N.; Hermann, P.; Lukeš, I. *Inorg. Chem.* **2009**, *48*, 455. (m) Kotková, Z.; Pereira, G. A.; Djanashvili, K.; Kotek, J.; Rudovský, J.; Hermann, P.; Vander Elst, L.; Muller, R. N.; Geraldes, C F G C.; Lukeš, I.; Peters, J. A. *Eur. J. Inorg. Chem.* **2009**, 119. (n) Giambastiani, G.; Oberhauser, W.; Bianchini, C.; Laschi, F.; Sorace, L.; Brueggeller, P.; Gutmann, R.; Orlandini, A.; Vizza, F. *Eur. J. Inorg. Chem.* **2005**, 2027. (o) Kong, D.; Xie, Y. *Inorg. Chim. Acta* **2002**, *338*, 142. (p) Campello, M. P. C.; Lacerda, S.; Santos, I. C.; Pereira, G. A.; Geraldes, C. F. G. C.; Kotek, J.; Hermann, P.; Vaněk, J.; Lubal, P.; Kubíček, V.; Tóth, É.; Santos, I. *Chem.—Eur. J.* **2010**, *16*, 8446. (q) Natrajan, L. S.; Khoabane, N. M.; Dadds, B. L.; Muryn, C. A.; Pritchard, R. G.; Heath, S. L.; Kenwright, A. M.; Kuprov, I.; Faulkner, S. *Inorg. Chem.* **2010**, *49*, 7700. (r) Szalay, P. S.; Zeller, M.; Hunter, A. D. *Acta Crystallogr., Sect. E: Struct. Rep. Online* **2011**, *67*, o644. (s) Bencini, A.; Bianchi, A.; Borselli, A.; Ciampolini, M.; Micheloni, M.; Paoli, P.; Valtancoli, B.; Dapporto, P.; Garcia-España, E.; Ramirez, J. A. *J. Chem. Soc., Perkin Trans. 2* **1990**, 209. (t) Táborskýa, P.; Lubala, P.; Havela, J.; Kotekb, J.; Hermannb, P.; Lukešb, I. *Collect. Czech. Chem. Commun.* **2005**, *70*, 1909.

(23) Dapporto, P.; Fusi, V; Giorgi, C.; Micheloni, M.; Palma, P.; Paoli, P.; Pontellini, R. *Supramol. Chem.* **1999**, 243.

(24) Lazar, I.; Hrncir, D. C.; Dae Kim, W.; Kiefer, G. E.; Sherry, A. D. *Inorg. Chem.* **1992**, *31*, 4422.

(25) Eliel, E. L.; Allinger, N. L.; Angyal, S. J.; Morris, G. A. *Conformational Analysis*; Interscience Publishers, Inc.: New York, 1965.

(26) Chválová, K.; Brabec, V.; Kaspárková, J. *Nucleic Acids Res.* **2007**, *6*, 1812−1821.

(27) Farrell, N.; Povirk, L. F.; Dange, Y.; DeMasters, G.; Gupta, M. S.; Kohlhagen, G.; Khan, Q. A.; Pommier, Y.; Gewirtz, D. A. *Biochem. Pharmacol.* **2004**, *5*, 857−866.

(28) Dapporto, P.; Formica, M.; Fusi, V.; Micheloni, M.; Paoli, P.; Pontellini, R.; Rossi, P. *Inorg. Chem.* **2000**, *39*, 4663.

(29) Fontanelli, M.; Micheloni, M. I. *Spanish-Italian Congr. Thermodynamics of Metal Complexes*, Peñiscola, Jun 3−6, 1990, University of Valencia: Spain, 1990; p 41.

(30) (a) Gran, G. *Analyst* **1952**, *77*, 661. (b) Rossotti, F. J.; Rossotti, H. *J. Chem. Educ.* **1965**, *42*, 375.

(31) Gans, P.; Sabatini, A.; Vacca, A. *Talanta* **1996**, *43*, 1739.

(32) Amatori, S.; Papalini, F.; Lazzarini, R.; Donati, B.; Bagaloni, I.; Rippo, M. R.; Procopio, A.; Pelicci, P. G.; Catalano, A.; Fanelli, M. *Lung Cancer* **2009**, *66*, 184−190.

(33) Kuykendall, J. R.; Trela, B. A.; Bogdanffy, M. S. *Mutat. Res.* **1995**, *343*, 209−218.

(34) CrysAlis CCD, Oxford Diffraction Ltd., Version 1.171.pre23_10 beta (release 21.06.2004 CrysAlis171.NET) (compiled Jun 21 2004,12:00:08).

(35) CrysAlis RED, Oxford Diffraction Ltd., Version 1.171.pre23_10 beta (release 21.06.2004 CrysAlis171.NET) (compiled Jun 21 2004,12:00:08).

(36) ABSPACK in CrysAlis RED, Oxford Diffraction Ltd., Version 1.171.29.2 (release 20−01−2006 CrysAlis171 .NET), (compiled Jan 20 2006,12:36:28).

(37) Altomare, A.; Cascarano, G. L.; Giacovazzo, C.; Guagliardi, A.; Burla, M. C.; Polidori, G.; Camalli, M. *J. Appl. Crystallogr.* **1999**, *32*, 115−119.

(38) Sheldrick, G. M. SHELX 97, University of Göttingen, Germany, 1997.

(39) Nardelli, M. *J. Appl. Crystallogr.* **1995**, *28*, 659−662.

(40) Macrae, C. F.; Bruno, I. J.; Chisholm, J. A.; Edgington, P. R.; McCabe, P.; Pidcock, E.; Rodriguez-Monge, L.; Taylor, R.; van de Streek, J.; Wood, P. A. *J. Appl. Crystallogr.* **2008**, *41*, 466−470.

(41) Farrugia, L. J. *J. Appl. Crystallogr.* **1997**, *30*, 565.

(42) (a) Binning, R.C.J..; Curtiss, L. A. *J. Comput. Chem.* **1990**, *11*, 1206. (b) Curtiss, L. A.; McGrath, M. P.; Blaudeau, J.-P.; Davis, N. E.; Binning, R. C. J.; Radom, L. *J. Chem. Phys.* **1995**, *103*, 6104. (c) McGrath, M. P.; Radom, L. *J. Chem. Phys.* **1991**, *94*, 511. (d) Frisch, M. J.; Pople, J. A.; Binkley, J. S. *J. Chem. Phys.* **1984**, *80*, 3265.

(43) Peng, C.; Ayala, P. Y.; Schlegel, H. B.; Frisch, M. J. *J. Comput. Chem.* **1996**, *17*, 49.

(44) Brooks, B. R.; Bruccoleri, R. E.; Olafson, B. D.; States, D. J.; Swaminathan, S.; Karplus, M. *J. Comput. Chem.* **1983**, *4*, 187.

(45) Accelrys, Inc., San Diego, CA.

(46) 2F8W: Narayana, N.; Shamala, N.; Ganesh, K. N.; Viswamitra, M. A. *Biochemistry* **2006**, *45*, 1200.